Preparation, Characterization, and Performance of Alumina-Supported Nanostructured Mo−Phosphide Systems

A. Montesinos-Castellanos,*,† T. A. Zepeda,‡,§ B. Pawelec,§ J. L. G. Fierro,§ and J. A. de los Reyes†

Área de Ingeniería Química, Universidad Autónoma Metropolitana-Iztapalapa, Avenida San Rafael Atlixco 186, Col. Vicentina, Iztapalapa, México DF, CP 09340, Centro de Ciencias de la Materia Condensada, Universidad Nacional Autónoma de México, Ensenada, BC, Mexico, CP 22800, Instituto de Catálisis y Petroleoquímica, Consejo Superior de Investigaciones Cientificas, c/Marie Curie 2, Cantoblanco, 28049 Madrid, Spain

Received July 10, 2007. Revised Manuscript Received August 22, 2007

A series of γ-Al_2O_3-supported molybdenum phosphide catalysts containing fixed Mo-loading (9.9 wt %) and variable P amounts (1.5−9.6 wt %) were prepared by temperature-programmed reduction (TPR) from their oxide precursors in hydrogen. The effect of the P/Mo atomic ratio on the structure of the molybdenum phosphide materials was studied by S_{BET}, XRD, HRTEM, TPD−NH_3, H_2 chemisorption, XPS, and ^{31}P- and ^{27}Al-MAS NMR techniques. The reactions involved in the transformation of oxide precursor to Mo−phosphide were followed by TPR. Specific surface areas of samples subjected to reduction at 1123 K were rather high (210−263 $m^2\ g^{-1}$). These catalysts were tested in the gas-phase hydrodesulfurization (HDS) of dibenzothiophene (DBT) at 553 K and 3.4 MPa. All Mo−phosphide catalysts were more active than a molybdenum sulfide sample with the same Mo-loading. The Mo−phosphide catalysts with P/Mo ratios of 1 and 1.1 were found to be the most active among the catalysts studied. The activity drop observed for higher P-loadings runs in parallel with the drop in specific areas. Moreover, the XPS and electrons diffraction analyses revealed the formation of MoP phase in all samples and the appearance of polyphosphates and $AlPO_4$ phases in P-rich ones. For the P-rich samples, the EFTEM study indicated that phosphate is accumulated around Mo atoms. It was found that the H_2 chemisorption capacity of the samples reduced at 1123 K correlates with the HDS performance of the catalysts.

1. Introduction

Over the past 10 years, the research community has shown an interest in studying the potential use of transition metal phosphides as hydrotreating catalysts.[1,2] This is because commercial molybdenum-sulfide-based catalysts have proven to be ineffective for deep hydrodesulfurization (HDS).[3,4] Recent works have shown that supported molybdenum phosphides (MoP) are several times more active for HDS and hydrodenitrogenation (HDN) reactions than supported MoS_2 catalysts.[1,2] Moreover, metal phosphides are more stable than sulfides during severe on-stream conditions.[5,6]

Molybdenum phosphides have a variety of interesting chemical and physical properties related to their metallic character that are similar to ordinary intermetallic compounds.[1] General information on synthesis methods and the nature and structure of metal phosphides were describe in a few reviews.[7−10] In short, MoP has a hexagonal tungsten carbide-type structure with space group P_{6m2} and bulk lattice parameters $a_0 = 322$ pm and $c_0 = 319$ pm.[1] In this structure, six P atoms trigonal-prismatically coordinate each Mo atom. Phosphorus is in reduced form in this phase, with the bonding ranging from ionic (P^{3+}) to metallic or covalent (P^0). Several reports have shown that the MoP catalysts (supported or unsupported) had an outstanding performance in HDS reactions.[11−13] A theoretical study by Liu and Rodriguez[14] shows that molybdenum phosphides show the largest reactivity toward CO and sulfur adsorption as compared to molybdenum nitrides and carbides. The latter information is very important regarding the catalytic response in the HDS reaction. From the combined activity and stability data, the

* Corresponding author. Tel.: (52) 5585022816, (52) 5558044900. e-mail: almo@xanum.uam.mx.
† Universidad Autónoma Metropolitana-Iztapalapa.
‡ Universidad Nacional Autónoma de México.
§ Consejo Superior de Investigaciones Cientificas.

(1) Oyama, S. T. *J. Catal.* **2003**, *216*, 343−352.
(2) Prins, R.; Pirngruber, G.; Weber, T. *Chimia* **2001**, *55*, 791−795.
(3) Topsøe, H.; Clausen, B. S.; Massoth, F. E. In *Hydrotreating Catalysts: Science and Technology*; Springer: Berlin 1996; p 310.
(4) Vasudevan, P. T.; Fierro, J. L. G. *Catal. Rev.−Sci. Eng.* **1996**, *38*, 161−188.
(5) Wang, X.; Clark, P.; Oyama, S. T. *J. Catal.* **2002**, *208*, 321−331.
(6) Wu, Z.; Sun, F.; Wu, W.; Feng, Z.; Liang, C.; Wei, Z.; Li, C. *J. Catal.* **2004**, *222*, 41−52.
(7) Aronsson, B.; Lundstrom, T.; Rundqvist, S. *Borides, Silicides and Phosphides*; John Wiley: New York, 1965.
(8) Corbridge, D. E. C. *Phosphorus, Studies in Inorganic Chemistry*; Elsevier: New York, 1990; p 10.
(9) Muetterties, E. L.; Sauer, J. C. *J. Am. Chem. Soc.* **1974**, *96*, 3410−3415.
(10) Henkes, A. E.; Vasquez, Y.; Schaak, R. E. *J. Am. Chem. Soc.* **2007**, *129*, 1896−1897.
(11) Stinner, C.; Prins, R.; Webber, Th. *J. Catal.* **2000**, *191*, 438−444.
(12) Stinner, C.; Prins, R.; Webber, Th. *J. Catal.* **2001**, *202*, 187−194.
(13) Cheng, R.; Shu, Y.; Li, L.; Zheng, M.; Wang, X.; Wang, A.; Zhang, T. *Appl. Catal., A* **2007**, *316*, 160−168.
(14) Liu, P.; Rodriguez, J. A. *Catal. Lett.* **2003**, *91*, 247−252.

10.1021/cm071814i CCC: $37.00
Published on Web 10/11/2007

authors concluded that the catalytic potential should increase following the sequence Mo < MoC ≈ MoN < MoP.[14]

Of course, the best option for achieving high dispersion of the MoP phase is supporting the Mo and P species on substrates with a high specific area, i.e., Al_2O_3. However, the strong active phase alumina interaction makes the synthesis of alumina-supported MoP more difficult than that of the unsupported ones.[15] Moreover, as a consequence of a strong metal-oxide-support interaction, the Mo oxide species supported on alumina are more difficult to reduce than those supported on a silica support.[16] Thus, there is a relatively larger body of literature devoted to silica-supported MoP[16−21] than to the alumina-supported ones.[21−23] A variety of techniques were employed in order to obtain useful information about the chemical states of P and Mo atoms in the supported MoP, such as ^{31}P MAS NMR,[20] XAFS,[23] XPS[19], and FTIR spectroscopy of adsorbed CO.[24] All these techniques confirmed the much easier transformation of the oxide precursors to the MoP phase on the SiO_2 supported catalysts with respect to those of the bulk ones.

Regarding the effect of P-loading, it is claimed that the synthesis of Ni_2P requires excess P.[25−28] This is because there are several intermediate phosphides, and phosphorus compounds (PH_3 and reduced P) are volatile at high temperatures.[15] Thus, it was found that the catalysts with a low P content develop $Ni_{12}P$ and metallic Ni on their support surface, whereas those with higher P content have the Ni_2P phase blocked by excess P.[28] One might deduce from the study by Sawhill et al.[25] that the optimization of P content depends on the support. This is because a large difference is found for the optimal P/Ni ratio of Ni_2P/SiO_2 (P/Ni = 0.8) and Ni_2P/Al_2O_3 (P/Ni = 2).[25] However, the XRD study on the Ni_2P/SiO_2 and Ni_2P/Al_2O_3 catalysts indicate that significant $Ni_{12}P_5$ impurities were present at lower P/Ni ratios in both SiO_2- and Al_2O_3-supported catalysts.[25] Contrary to Ni_2P systems, and to the best of our knowledge, there are no reports on the effect of P loading on the catalytic performance of alumina-supported MoP catalysts. This is probably because the alumina material has a strong affinity for phosphates. Thus, for P-rich catalysts, one might expect the formation of a strongly bound amorphous phosphate surface layer on the alumina support.[22]

Within the above framework, the purpose of this study is to compare the surface properties of the alumina-supported MoP catalysts with varying P content. A series of MoP/Al_2O_3 catalysts with P/Mo ratios ranging from 0.5 to 3.0 were prepared by temperature-programmed reduction of the oxide precursors in H_2 at 1123 K. The final catalyst morphology was studied by different techniques (N_2 adsorption−desorption isotherms, X-ray diffraction, high-resolution transmission electron microscopy (HRTEM), magic angle spinning-nuclear magnetic resonance (MAS NMR), X-ray photoelectron spectroscopy (XPS), and hydrogen chemisorption). The catalytic response of the synthesized materials was tested in the gas-phase HDS reaction of DBT and compared to that of a conventional MoS_2/Al_2O_3 catalyst.

Table 1. Composition[a] and Labeling for MoP/Al_2O_3 Catalysts

sample	Mo (wt %)	P (wt %)	P/Mo ratio
$MoP_{(0.5)}/Al$	9.9	1.5	0.5
$MoP_{(1)}/Al$	9.9	3.2	1
$MoP_{(2)}/Al$	9.9	6.7	2
$MoP_{(3)}/Al$	9.9	9.6	3
MoS_2/Al	9.9		
P/Al		6.3	

[a] The number in parentheses indicates the P/Mo ratio.

2. Experimental Section

2.1. Catalyst Preparation. The Al_3O_3 support (provided by the Instituto Mexicano del Petróleo (IMP)) was calcined at 1173 K prior to catalyst preparation. The phosphate precursors were prepared by impregnation of the γ-Al_3O_3 support using the pore filling method. The chemical composition and catalyst labeling are given in Table 1. The precursors for Mo and P were $(NH_4)_6Mo_7O_{24}\cdot 4H_2O$ and $(NH_4)_2HPO_4$, respectively. The aqueous solution of $(NH_4)_2HPO_4$ was prepared with variable concentrations in order to obtain selected Mo/P molar ratios in the final catalyst. For the sake of clarity, the prepared MoP/Al_2O_3 catalysts were denoted as MoP_x/Al, where x is the P/Mo molar ratio. The impregnates were dried at 393 K and then calcined at 823 K under an air flow. The precursor was subsequently ground in a mortar and pestle and sieved through a 80/100 mesh. To convert the phosphate into phosphide, we reduced the catalyst oxide precursors under a hydrogen flow (1500 NTP $cm^3\ g^{-1}\ min^{-1}$) by temperature-programmed reduction to 1123 K (rate of 5 K min^{-1}) and then isothermally reduced them at this temperature for 2 h. After reduction, the MoP catalyst was cooled to room temperature under a He flow. The hydrogen used for precursor reduction, and all the inert gases used during sample transfer for catalyst characterization were of the highest purity in order to prevent pyrophoric oxidation of the synthesized phosphide catalysts upon possible contact with parts per million of O_2.

Two reference MoS_2/Al_2O_3 and P/Al_2O_3 catalysts were prepared by the same method as described above for the oxide precursors of MoP/Al_2O_3 catalysts. The MoS_2/Al_2O_3 sample with 9.9 wt % Mo (henceforth referred to as MoS_2/Al) was prepared by sulfidation of the P-free Mo/Al_2O_3 catalyst at 673 K for 1 h in a 15% H_2S/H_2 flow. The conditions of catalyst drying and calcination were the same as described above for the oxide precursors of MoP/Al_2O_3 catalysts. The alumina-supported phosphorus catalyst (henceforth referred to as P/Al) containing 6.3 wt % P was prepared by impregnation of alumina material with the aqueous solution of $(NH_4)_2HPO_4$, followed by catalyst drying, calcination, and further

(15) Zuzaniuk, V.; Prins, R. *J. Catal*. **2003**, *219*, 85−96.
(16) McCrea, K. R.; Logan, J. W.; Tarbuck, T. L.; Heiser, J. L.; Bussel, M. E. *J. Catal.* **1997**, *171*, 255−267.
(17) Li, W.; Dhandapani, B.; Oyama, S. T. *Chem. Lett.* **1998**, 207−208.
(18) Clark, P.; Wang, X.; Deck, P.; Oyama, S. T. *J. Catal.* **2002**, *210*, 256−265.
(19) Phillips, D. C.; Sawhill, S. J.; Self, R.; Bussell, M. E. *J. Catal*. **2002**, *207*, 266−273.
(20) Clark, P.; Wang, X.; Oyama, S. T. *J. Catal.* **2002**, *207*, 256−265.
(21) Rodriguez, J. A.; Kim, J.-Y.; Hanson, J. C.; Sawhill, S. J.; Bussel, M. E. *J. Phys. Chem. B* **2003**, *107*, 6276−6285.
(22) Clark, P. A.; Oyama, S. T. *J. Catal.* **2003**, *218*, 78−87.
(23) Oyama, S. T.; Clark, P.; Teixeira da Silva, V. L. S.; Lede, E. J.; Requejo, F. G. *J. Phys. Chem. B* **2001**, *105*, 4961−4966.
(24) Wu, Z.; Sun, F.; Wu, W.; Feng, Z.; Liang, C.; Wei, Z.; Li, C. *J. Catal.* **2004**, *222*, 41−52.
(25) Sawhill, S. J.; Layman, K. A.; Van Wyk, D. R.; Engelhard, M. H.; Wang, Ch.; Bussell, M. E. *J. Catal.* **2005**, *231*, 300−313.
(26) Oyama, S. T.; Wang, X.; Lee, Y.-K.; Chun, W.-J. *J. Catal.* **2004**, *221*, 263−273.
(27) Stinner, C.; Tang, Z.; Haouas, M.; Weber, Th.; Prins, R. *J. Catal.* **2002**, *208*, 456−466.
(28) Oyama, S. T.; Wang, X.; Lee, Y.-K.; Bando, K.; Requejo, F. G. *J. Catal.* **2002**, *210*, 207-.217.

reduction with H_2 at conditions described above for MoP/Al_2O_3 catalysts.

2.2. Catalyst Characterization. *2.2.1. N_2 Adsorption−Desorption Isotherms.* Nitrogen adsorption−desorption isotherms were obtained at 77 K on an Autosorb Quantachrome apparatus. Prior to the experiments, the MoP/Al samples were degassed at 543 K in a vacuum for 5 h. Specific surface area (S_{BET}) was calculated by the BET equation applied to the range of relative pressures $0.05 < P/P^0 < 0.30$. Average pore diameter was calculated by applying the Barret−Joyner−Halenda method (BJH) to the adsorption branches of the N_2 isotherms. Cumulative pore volume was obtained from the isotherms at $P/P^0 = 0.99$.

2.2.2. Temperature-Programmed Reduction. TPR profiles were obtained on an ISRI RIG 100 apparatus equipped with a thermal conductivity detector (TCD). Prior to the analyses, the samples were dried with Ar at 393 K for 4 h and then reduced in flowing gas containing 10% H_2/Ar, raising the temperature from 373 K to a final temperature of 1223 K at a rate of 10 K min^{-1}.

2.2.3. Nuclear Magnetic Resonance. One-pulse solid-state nuclear magnetic resonance (NMR) spectra were obtained under magic angle spinning (MAS) conditions using a Bruker ASX-300 spectrometer with a magnetic field strength of 7.05 T, corresponding to a ^{31}P Larmor frequency of 121.4 MHz. The spectra were obtained with a sample spinning rate of 5 kHz. The chemical shifts were referenced to a H_3PO_4 solution (85%). The ^{27}Al MAS NMR spectra were obtained operating the spectrometer at 78.3 MHz. The calibrated $\pi/2$ pulse was 2 μs, and the recycle time used was 0.5 s. The ^{27}Al chemical shifts were referenced using an aqueous solution of $Al(NO_3)_3$ as the external standard. To collect the NMR data from the reduced samples, they were placed in a glove box under Ar and packed in ZrO_2 rotors immediately after preparation. The time for recording one NMR spectrum was 10 min.

2.2.4. X-ray Diffraction. X-ray diffractograms for freshly reduced MoP samples were recorded on a Siemens D500 diffractometer, using monochromatic Cu K_α radiation ($\lambda = 0.1541$ nm). The K_α radiation was selected with a diffracted beam monochromator.

2.2.5. High-Resolution Transmission Electron Microscopy. Microscope equipped with an ultra-high-resolution pole piece ($\lambda =$ 0.00251 mm, resolution of 0.17 nm). The appropriate software (GATAN) was used to obtain interplanar distances and particle size.

2.2.6. X-ray Photoelectron Spectroscopy. The X-ray photoelectron spectra of the freshly reduced catalysts were recorded with a VG Escalab 200R spectrometer equipped with a hemispherical electron analyzer and an Mg Kα ($h\nu = 1253.6$ eV) X-ray source. The freshly ex situ reduced catalysts were kept under *i*-octane in order to avoid exposure to air and then introduced into the preparation chamber. All catalysts were degassed at 1×10^{-5} mbar and then transferred to the ion-pumped analysis chamber, where residual pressure was kept below 7×10^{-9} mbar during data acquisition. The binding energies (BE) were referenced to the C 1s peak (284.9 eV) to account for the charging effects. The areas of the peaks were computed after fitting of the experimental spectra to Gaussian/Lorentzian curves and removal of the background (Shirley function).

2.2.7. Temperature-Programmed Desorption of NH_3. The acid strength of the oxide catalysts was determined by TPD−NH_3 measurementsusing a Micromeritics TPD/TPR 2900 device. The freshly reduced sample (0.05 g) was first degassed in a He flow (Air Liquide, 99.996%) at 483 K for 1 h and then ammonia-saturated by a flowing 5% NH_3/He stream at 373 K for 0.5 h. The physically adsorbed NH_3 was then removed by treatment in a He flow for 0.5 h at 353 K. The TPD−NH_3 experiments were performed by heating the sample at a linear rate of 15 K min^{-1} from 353 to 1050 K, while recording ammonia desorption by TCD.

2.2.8. Chemisorbed H_2 Measured. Metal dispersion was determined from the amount of chemisorbed H_2 measured with a pulse method using a Micrometrics 2900 apparatus. Prior to chemisorption measurements, the oxide precursor (ca. 50 mg) was reduced in situ in a H_2/Ar stream, as described above in the catalyst preparation section, and then cooled in an Ar flow in order to remove physisorbed hydrogen. Pulses (0.113 mL) of 10% H_2/Ar were injected into a stream of Ar carrier gas (50 mL min^{-1}) and contacted with the catalyst at room temperature. Metal dispersion was calculated assuming that one Mo atom chemisorbs one hydrogen atom.

2.2.9. Catalytic Activity Measurements. The HDS of DBT (Aldrich; 99.9%) was carried out in a continuous-flow microreactor in the vapor phase working at 553 K and hydrogen pressure of 3.4 MPa. First, the oxide precursors were reduced at 1123 K for 2 h at a rate of 5 K min^{-1} under a hydrogen flow (1500 NTP cm^3 g^{-1} min^{-1}). The high heating rate and hydrogen flow rate were used to remove local moisture from the surface of the precursor.[29] Following pretreatment, the catalyst (50 mg) was placed inside the reactor under Ar. Subsequently, the temperature and pressure were adjusted to the chosen reaction conditions. Before reaction, the sulfide MoS_2/Al_2O_3 catalyst was activated by in situ sulfidation of the P-free Mo/Al_2O_3 catalyst with 15% H_2S/H_2 mixture at 673 K for 1 h. To compare catalyst activity, we performed two sets of experiments. On the one hand, activity tests were performed keeping DBT conversion below 15% (differential reaction mode). In this case, DBT concentration in the feed was adjusted for each catalyst (a total flow in the range of 6−10 L h^{-1}). On the other hand, the stability of the catalysts was compared employing the same DBT concentration (pDBT = 15 kPa) in the feed. The products were analyzed in a gas chromatograph equipped with a flame ionization detector (FID) and a capillary column of 5% phenyl−95% methylpolysiloxane (EC5), purchased from Alltech. Dibenzothiophene HDS activities (mol of DBT g_{cat}^{-1} s^{-1}) were calculated from the total product peak areas calculated from the chromatogram after 100 h of reaction time. The specific reaction rates were calculated according to the following expression

$$\text{specific reaction rate} = \frac{\text{molar flow rate of DBT}}{\text{catalyst mass}} (\text{DBT conversion})$$

3. Results and Discussion

A series of MoP/Al_2O_3 catalysts were prepared in this study by means of the temperature-programmed reduction of their oxide precursors under hydrogen flow up to a final reduction temperature of 1123 K and were kept at this temperature for 2 h. A relatively low Mo content (9.9 wt %) was employed in order to achieve homogeneous Mo dispersion and taking into account that the catalytic activity of those systems was found to be independent of the amount of MoP deposited on the alumina surface and independent of the presence of X-ray visible bulk MoP.[22]

The textural properties of such prepared catalysts were studied by N_2 adsorption−desorption isotherms at 77 K. All adsorption−desorption isotherms (not shown here) were of type IV of IUPAC classification with a sharp step at intermediate relative pressures. The appreciable type H1 hysteresis loops indicate the presence of textural mesopores and cylindrical pores. The effect of P-concentration on the specific catalyst surface area was estimated using the classical

(29) Wang, A.; Ruan, L.; Teng, Y.; Li, X.; Li, M.; Ren, J.; Wang, Y.; Hu, Y. *J. Catal.* **2005**, *229*, 314−321.

Table 2. Textural Properties,[a] Crystallite Size,[b] and Metal Dispersion[c] for Freshly Reduced MoP/Al_2O_3 Catalysts

samples	S_{BET} (m^2g^{-1})	V_{total} (cm^3g^{-1})	d (nm)	crystallite size (nm)	H_2 uptake[c] (μmol/g_{cat})	dispersion[c] (%)	Mo/Al atomic ratio[d]
$MoP_{(0.5)}$/Al	263	263	8.0	4.2 ± 0.2	31.5	6.1	0.015
$MoP_{(1)}$/Al	215	215	6.7	4.1 ± 0.1	61.5	11.5	0.021
$MoP_{(2)}$/Al	212	212	6.5	4.9 ± 0.2	37.5	7.2	0.017
$MoP_{(3)}$/Al	210	210	5.7	5.0 ± 0.3	24.9	4.8	0.018

[a] Specific BET surface area (S_{BET}), total pore volume (V_{total}), and pore diameter (d) as determined by N_2 adsorption−desorption isotherms at 77 K. [b] As determined by HRTEM. [c] Chemisorption capacity and metal dispersion as determined by pulse method of H_2 chemisorption. [d] Mo/Al atomic ratio measured by XPS.

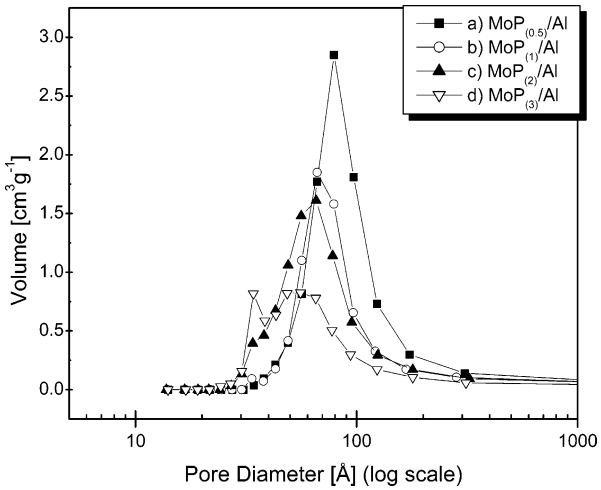

Figure 1. BJH pore size distributions, as determined from adsorption branch of N_2 isotherm, for MoP/γ-Al_2O_3 catalysts reduced at 1123 K.

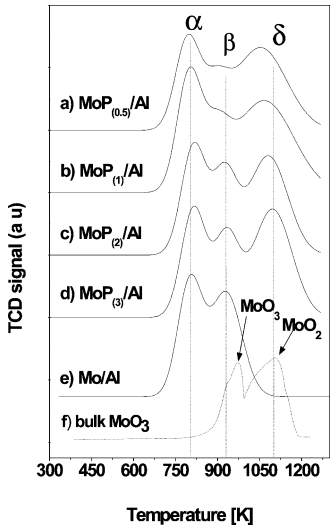

Figure 2. TPR profiles of the oxide precursors.

Brunauer−Emmett−Teller (BET) method. The pure γ-Al_2O_3 support shows a specific area of 304 m^2 g^{-1} and a total pore volume of 0.94 cm^3 g^{-1}. The specific area (S_{BET}), total pore volume ,and average pore diameter of the freshly reduced MoP/Al_2O_3 catalysts are compiled in Table 2. As expected, all catalysts reveal a lower S_{BET} specific area with respect to pure support, although their areas still remain high (in the range 263−210 m^2 g^{-1}). This is due to the metal dilution effect, as well as to the modification of pore opening by deposition of Mo/P species on the carrier surface. Both S_{BET} specific area and total pore volume show similar trends ($MoP_{(0.5)}$/Al > $MoP_{(1)}$/Al ≈ $MoP_{(2)}$/Al ≈ $MoP_{(3)}$/Al), indicating that for the two latter catalysts the excess of P might be located on the external catalyst surface. This could also be deduced from similar S_{BET} values (215−210 m^2 g^{-1}) of the $MoP_{(2)}$/Al and $MoP_{(3)}$/Al) catalysts.

All catalysts show a similar and relatively narrow pore distribution. The BJH pore diameter distributions of the catalysts derived from the adsorption branch of the N_2 adsorption isotherms are displayed in Figure 1. As seen, all synthesized catalysts are mesoporous and their pore diameter is in the range 5.7−8.0 nm (Table 2). Considering the average pore diameter values compiled in Table 2, one might note that an increase in P loading led to a decrease in the average pore diameter of the catalysts. One important point is that the catalysts with lowest P content have the same average pore diameter as that of pure support (8.0 nm), indicating the location of guest phosphate on the external catalyst surface. The $MoP_{(3)}$/Al sample is unique among the catalysts studied, with bimodal BJH pore distribution indicating that high P loading decreases the structure parameters (S_{BET}, pore diameter, and total pore volume). This is probably because the P species located on the external catalyst surface blocks the small pores.[29,30]

Because all catalysts show a slightly larger pore dimension (5.7−8.0 nm) as compared to average particle sizes derived from HRTEM (4.0−5.3 nm), the possible location of some metallic particles within their pore network was estimated using an equation proposed by Vradman et al.[31]

$$NS_{BET} = S_{BET\ of\ catalyst}/[(1 - y)\, S_{BET\ of\ support}]$$

where NS_{BET} is normalized S_{BET} and the weight fraction of theguest phases. For all catalysts, the normalized surface area calculated from this equation follows the trend $MoP_{(0.5)}$/Al (0.98) > $MoP_{(3)}$/Al (0.86) > $MoP_{(2)}$/Al (0.84) > $MoP_{(1)}$/Al. (0.81). Thus, the NS_{BET} below 1 for the three latter catalysts reflects some blocking of the alumina pores with the guest particles located inside them.

TPR is a powerful tool for studying the reduction behavior of supported phases. Moreover, in some cases, the reduction profiles of oxide precursors provide useful information about the degree of interaction of the supported phase with the support. Thus, in order to investigate the reactions involved in MoP formation, the oxide precursors were studied by TPR technique. The TPR profiles of the synthesized oxide precursors are shown in plots a and b in Figure 2. For comparison purposes, the TPR profiles of the P-free Mo/Al_2O_3 catalyst and bulk MoO_3 compound are also included in this figure. The TPR profile of the bulk MoO_3 displays two reduction peaks at 975 and 1114 K (Figure 2f), which

(30) Iwamoto, R.; Grimblot, J. *Adv. Catal*. **2000**, *44*, 417−503.
(31) Vradman, L.; Landau, M. V.; Kantorovich, D.; Koltypin, Y.; Gedanken, A. *Microporous Mesoporous Mater*. **2005**, *79*, 307−318.

Scheme 1. Plausible Representation of Active Phase Formation for Low-P-Content Catalysts, as Described by δ Reduction Process (from TPR)

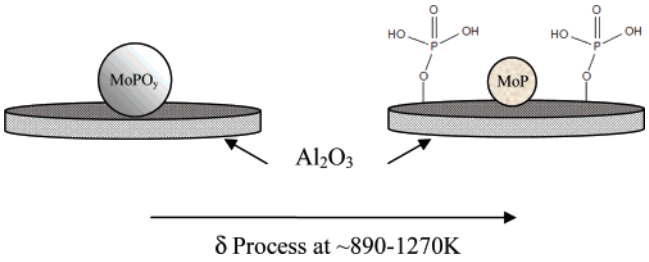

Scheme 2. Plausible Representation of Active Phase Formation for P-Rich Catalysts, as Described by δ Reduction Process (from TPR)

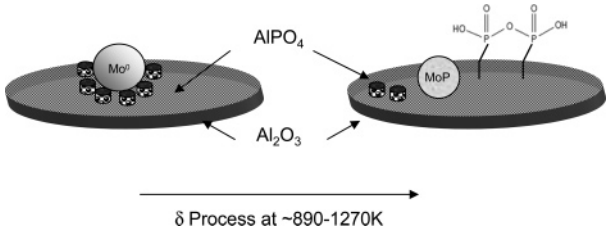

correspond to the two-step MoO_3 phase reduction ($MoO_3 \rightarrow MoO_2 \rightarrow Mo^0$).[22] For the P-free Mo/Al_2O_3 sample (Figure 2e), those two reduction steps occur at much lower temperatures (808 and 929 K, respectively), indicating the easier reduction of MoO_3 species when supported on alumina with respect to unsupported ones. Regardless of P content, the TPR profiles of all oxide precursors show three peaks at ca. 800, 930, and 1098 K, which will be labeled henceforth as α, β, and δ, respectively. For the samples with low P content (parts a and b in Figure 2), the TPR profiles show well-resolved α and δ peaks and the absence of β peak. Contrary to those catalysts, the sample with largest P contents (parts c and d in Figure 2) showed a well-resolved β-peak and its intensity increases with increasing P content. TPR results showed that reduction processes were a function of the P content. Probably in Mo-rich samples, the reduction to MoP phase proceeded by direct reduction of Mo and/or phosphates species, and in P-rich samples, reduction proceeded by reduction of AlPO phase and then the reduction of Mo and P species for produce MoP phase.

Because all catalysts studied here show good active phase dispersion, one might suppose that Mo−O−Al linkages are developed. However, this is hardly possible considering the EXAFS study performed by Oyama et al.[23] on in situ reduced (1123 K) MoP/Al_2O_3 catalysts. For catalysts with high and low P content, the plausible representations of MoP phase formation by δ reduction process (reduction in temperature range 890−1270 K) are shown in Schemes 1 and 2, respectively. For the $MoP_{(0.5)}$/Al and $MoP_{(1)}$/Al catalysts, the $MoPO_y$ phases are reduced to MoP, and some P atoms present on the catalyst surface as monophosphate species surround the MoP particles (Scheme 1). On the other hand, for $MoP_{(2)}$/Al and $MoP_{(3)}$/Al catalysts, some $AlPO_4$ species and polyphosphates surrounding MoP particles are expected after reduction in the temperature range of 890−1270 K (Scheme 2). Comparing the crystallite sizes summarized in Table 2, the P-rich catalysts show a slightly larger crystallite size than the P-poor ones (5 ± 0.3 nm vs 4.1 ± 0.1 nm). On the basis of the ^{27}Al MAS NMR results discussed below, this is probably due to a drop in the metal−support interaction linked with the presence of $AlPO_4$ phase on the surface of P-rich catalysts. Accordingly, one might assume that the $AlPO_4$ phase is located between Mo and the carrier in $MoP_{(2)}$/Al and $MoP_{(2)}$/Al samples promoting crystal growth, as outlined in Scheme 2, whereas the surface of catalysts with low P content have MoP and polyphosphate phases.

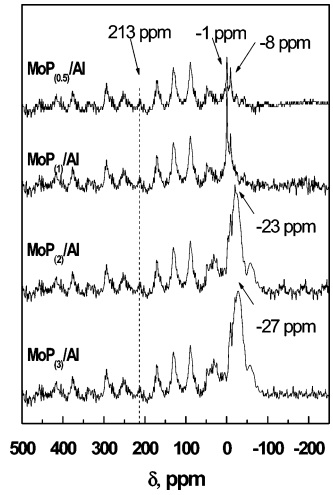

Figure 3. ^{27}Al MAS NMR spectra of the MoP/γ-Al_2O_3 catalysts reduced at 1123 K.

To identify the phases formed and study the structure and bonding in the materials, we studied the freshly reduced alumina-supported MoP catalysts by ^{31}P and ^{27}Al MAS NMR techniques. Figure 3 shows the ^{31}P MAS NMR spectra of the catalysts obtained at the same sample's rotation speed. As seen in this figure, and irrespectively of P content, all NMR spectra displayed a very complex pattern. This is a consequence of the considerable anisotropy surrounding the P atom. For the phosphides, the measured NMR shift is a Knight shift resulting from the interaction of P nuclei with the conduction electron of the solid.[1] In this study, ^{31}P MAS NMR spectra of all samples showed one isotropic peak at 213 ppm, which is attributed to the molybdenum phosphide phase, and it is similar to the ^{31}P NMR signal reported previously for MoP/SiO_2 catalysts.[20]

The ^{31}P NMR spectra showed that the MoP phase was effectively formed on alumina support; no resonances for other phosphides, such as MoP_2, MoP_4, Mo_3P, Mo_4P_3, Mo_8P_5, etc., were detected. Several other peaks located at −1, −8, −23, and −27 ppm are characteristic resonances for phosphate species. Monophosphates were identified on lower-P-content samples ($MoP_{(0.5)}$/Al and $MoP_{(1)}$/Al). Monophosphates could be an unreactive phase in HDS reaction. The presence of phosphates indicates that samples were exposed to parts per million of O_2 regardless of the fact that a glove box with Ar was used for protecting the catalyst during its transfer from the pretreatment reactor to ZrO_2 rotors. However, pyrophoric sample oxidation was minimal as no phosphide peaks were observed for samples reduced at 1123 K and then passivated (spectra not shown here). Thus,

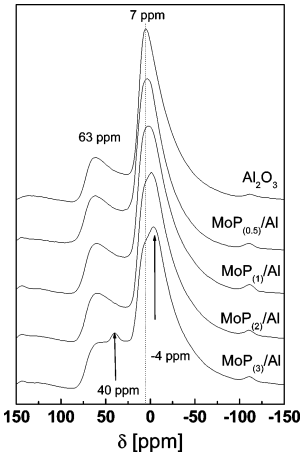

Figure 4. Powder X-ray diffraction patterns of the reduced MoP/γ-Al_2O_3 catalysts.

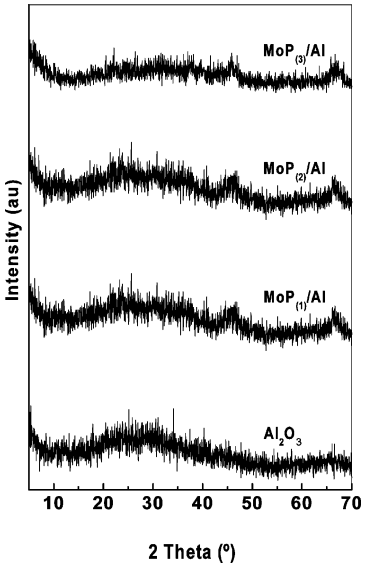

Figure 5. ^{31}P MAS NMR spectra of the MoP/γ-Al_2O_3 catalysts reduced at 1123 K.

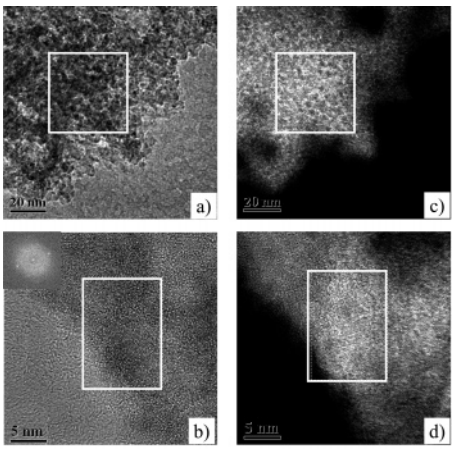

Figure 6. Micrograph of the $MoP_{(3)}$/Al sample reduced at 1123 K. (a, b) Bright-field and (c, d) filtering P signal (132 eV). Inset of b is the diffraction pattern of MoP phase ([103] plane).

oxidation of phosphides into phosphate might well take place along the transfer step. The catalysts with high P content show the phosphate signal shifted to stronger fields (−23 and −27 ppm).

In close agreement with other studies,[32,33] the $AlPO_4$ phase was detected by ^{31}P and ^{27}Al MAS NMR on the surface of the P-rich catalysts ($MoP_{(2)}$/Al and $MoP_{(3)}$/Al). The formation of $AlPO_4$ and polyphosphates in P-loaded alumina has been reported previously.[30] Figure 4 shows ^{27}Al MAS NMR spectra of the catalysts together with those of bare alumina. All spectra show resonances for tetrahedral and octahedral aluminum ions. ^{27}Al MAS NMR spectra for the catalysts with lower P content exhibited the same pattern as that of pure alumina. The tetrahedral and octahedral peaks for Al_2O_3 are located at ∼65 and ∼ 6 ppm, respectively.[32] For the catalysts with higher P content, the ^{27}Al spectra show a shift of the octahedral resonance at −4 ppm. Additionally, the ^{27}Al NMR spectrum of the $MoP_{(3)}$/Al sample with largest P content shows one peak at 40 ppm, indicating the presence of $AlPO_4$ phase with tetrahedral coordination of its Al-atom. Finally, additional ^{27}Al and ^{31}P NMR spectra reveal that the P/Al sample reduced at temperatures below 1123 K has the characteristic peaks of the $AlPO_4$ phase (spectra not shown here). These results suggest that the $AlPO_4$ phase formed upon calcination remains on the catalyst surface after oxide precursor reduction at 1123 K. For the P/Al sample, the $AlPO_4$ phase was detected when P content was of 6.3 wt %, whereas for MoP/Al catalysts, this phase was detected when P content was higher than 6.7 wt %. Thus, in close agreement with the TPR results discussed above, the NMR study suggests the inhibition of the $AlPO_4$ phase formation when both Mo and P species are present on the surface of calcined catalyst.

The MoP catalysts were studied by XRD in order to identify crystal phases formed after oxide precursor reduction at 1123 K. Figure 5 shows the XRD patterns of the MoP/Al_2O_3 catalysts, showed within the diffraction angle range $2\theta = 5-80°$. As seen in this figure, the XRD patterns of all catalysts are practically the same and similar to that of bare alumina. Thus, the X-ray measurements indicate that the phases formed were amorphous or their size was below the detection limit of the X-ray instrument (ca. 4 nm). Thus, the HRTEM and electron diffraction techniques were employed in order to estimate the crystallite sizes and evidence the formation of MoP, respectively, after H_2-reduction of the oxide precursors at 1123 K. For all catalysts, HRTEM micrographs (not shown here) display very well dispersed particles with a globular shape. This globular form of the particles is a well-known feature of metal phosphides, as reported previously for MoP/SiO_2 catalysts.[19] The main particle sizes, as calculated from particle size distribution (not shown here) obtained from TEM images, are summarized in Table 2. As indicated in this table, the mean particle sizes of all catalysts were in the range 4.0−5.3 nm.

The energy-filtered transmission electron microscopy (EFTEM) technique was used for studying the $MoP_{(3)}$/Al sample with the largest P-content (9.6 wt %). Figure 6a−d shows several micrographs of this catalyst; bright-field images (images a and b in Figure 6) are compared with those of the dark-field image (images c and d in Figure 6), filtering

(32) Quartararo, J.; Guelton, M.; Rigole, M.; Amoureux, J. P.; Fernandez, Ch.; Grimblot, J. *J. Mater. Chem.* **1999**, *9*, 2637−2646.
(33) Yang, S.; Liang, C.; Prins, R. *J. Catal.* **2006**, *237*, 118−130.

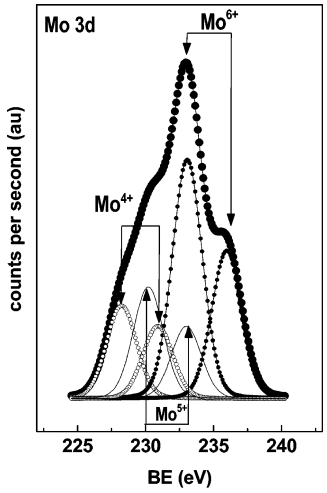

Figure 7. Mo 3d core level spectra of the freshly reduced $MoP_{(1)}$/Al catalyst.

P signal at 132 eV). We can observe that strong contrast points in the bright-field image (Figure 6a) correspond to bright points in the dark-field image (Figure 6c). One might reach the same conclusion by comparing images b and d in Figure 6. This observation indicates that P-atoms are present in the close vicinity of Mo atoms. Indeed, ^{31}P MAS NMR results showed that some P atoms on the $MoP_{(3)}$/Al sample are present forming molybdenum phosphide phase, and some P is present as phosphate.

It is well-known that the surface exposure of the metal species depends, in part, on metal−support interaction. On the basis of TPR results, a strong metal−alumina support interaction appears to have developed. This was also confirmed by the XPS technique, which provides useful information about the chemical state of the elements and their surface exposure after precursor reduction at 1123 K. As an example, the Mo 3d core-level spectra of the $MoP_{(1)}$/Al sample are shown in Figure 7. As seen in this figure, peak deconvolution reveals three doublets, indicating the presence of Mo^{6+}, Mo^{5+}, and Mo^{4+} species. The most intense Mo $3d_{5/2}$ peak of the first doublet located at 232.8 eV indicates the presence of Mo^{6+} species, whereas the $Mo3d_{5/2}$ component of the second doublet at 230.2 eV lies in the range reported by others for Mo^{5+} species. Finally, the $Mo3d_{5/2}$ component of the third doublet with BE at 229.6 eV is indicative of Mo^{4+} species.[34] Our XPS study is therefore consistent with that reported by Phillips et al.[19] for the MoP/SiO_2 system. In their study, a binding energy of 228.4 eV was assigned to a CUS $Mo^{\delta+}$ surface site ($0 < \delta \leq 4$) species. Similarly, the IR spectroscopy study of MoP/SiO_2 catalysts by CO probing demonstrated the presence of CUS $Mo^{\delta+}$ surface sites ($3 < \delta < 5$) after precursor reduction at 923 K.[24] Thus, although MoP is considered to have a metallic character,[7−9] our XPS study on MoP/Al catalysts indicate that the Mo atoms in the molybdenum phosphide phase are positively charged due to the charge transfer from Mo to the electronegative P atoms. A similar conclusion was advanced by Wu et al.[24] from their IR study on MoP/SiO_2 catalysts, as the P 2p region shows a peak with a binding energy of 134.0 eV, indicative of surface PO_4^{3-} species.[19,35,36] These BE values are much lower than those of 135.2 eV corresponding to the P_2O_5 phase,[34] indicating that the phosphorus species are strongly interacted with the alumina support. Thus, considering combined NMR and XPS results, it is more likely that the MoP phase is covered by a phosphide layer. Finally, the XPS technique proved that P-loading influenced the Mo species surface exposure. Considering the Mo/Al atomic ratio (Table 2), the surface exposure of Mo species follows the trend: $MoP_{(1)}/Al > MoP_{(3)}/Al \approx MoP_{(2)}/Al > MoP_{(0.5)}/Al$.

The presence of both Lewis and Brønsted acid sites on γ-Al_2O_3 has been reported.[37] In addition, one might expect an increase in acidity upon phosphorus addition to alumina[30] and upon high-temperature pretreatment,[38] P species induced acidity by contacting with alumina surface, even if they are not always highly acidic by themselves. Thus, to compare catalyst acidity, we carried out the TPD−NH_3 study on the samples reduced in situ at 1123 K; the results are shown in Figure 8 a and the representative deconvolution of the TPD−NH_3 profile of the $MoP_{(1)}$/Al sample in Figure 8b. Considering that the final surface acidity of the catalyst depends on the evolution of the metal−support interaction during the reduction step,[39] catalyst acidity was evaluated for the freshly reduced catalysts. As seen in Figure 8, the TPD−NH_3 profiles of all Mo phosphide catalysts are similar. The total acidity of the samples, calculated as the sum of the weak, medium, and strong acid sites obtained after fitting of the experimental curves by Gaussian deconvolution (not shown here), are listed in Table 3. Total acidity of catalysts follows the trend $MoP_{(2)}/Al > MoP_{(3)}/Al > MoP_{(0.5)}/Al > MoP_{(1)}/Al$. As expected, both $MoP_{(2)}$/Al and $MoP_{(3)}$/Al catalysts show larger total acidity than the $MoP_{(0.5)}$/Al and $MoP_{(1)}$/Al catalysts. For the phosphate-containing catalysts, it was reported that P loading on alumina leads to an increase in the number of Brønsted acid sites, whereas the amount of Lewis acid sites remains almost unchanged.[40] This is because at low concentration, phosphoric acid forms $P{\equiv}(O-Al)_3$ bonds with the OH groups on the alumina surface, but only single $P(OH)_2-O-Al$ occurs at high concentration, and hence the Brønsted acidity of the catalyst increases. Therefore, for the P-rich catalysts with phosphate species on the surface, the increase in acidity is due to the formation of $P(OH)_2-O-Al$ bonds or even to free $OP(OH)_3$ entities interacting with the alumina surface via H-bonding. In agreement with the literature,[41] we found that the incorporation of phosphorus in γ-Al_2O_3 reduces the number of strong acid sites and increases the number of medium strength acid sites. For example, the number of strong acid sites for $MoP_{(1)}$/

(34) Briggs, D.; Seah, M. P., Eds. In *Practical Surface Analysis. Auger and X-ray Photoelectron Spectroscopy*; Wiley: New York, 1990.
(35) Okamoto, Y.; Nitta, Y.; Imanaka, T.; Teranishi, S. *J. Catal.* **1980**, *64*, 397−404.
(36) Okamoto, Y.; Fukino, K.; Imanaka, T.; Teranishi, S. *J. Catal.* **1982**, *74*, 173−182.
(37) Zhang, W.; Smirniotis, P. G. *Appl. Catal., A* **1998**, *168*, 113−130.
(38) Shen, Y.; Suib, S. L.; Deeba, M.; Koermer, G. S. *J. Catal.* **1994**, *146*, 483−490.
(39) Scheffer, B.; Molhoek, P.; Moulijn, J. A. *Appl. Catal.* **1989**, *46*, 11−30.
(40) Fitz, C. W.; Rase, H. F. *Ind. Eng. Chem. Prod. Res. Dev.* **1983**, *22*, 40−44.
(41) Stanislaus, A.; Absi-Halabi, M.; Al-Dolama, K. *Appl. Catal.* **1988**, *39*, 239−253.

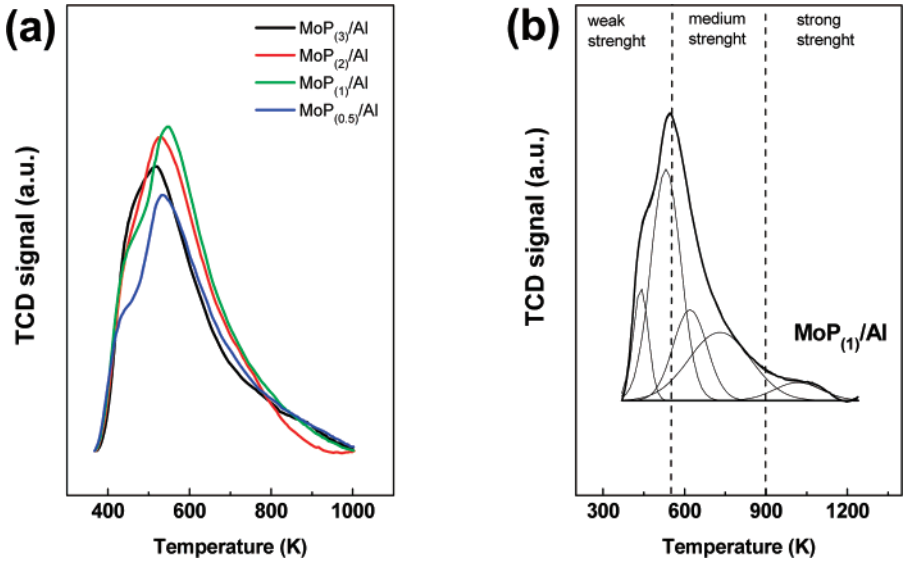

Figure 8. TPD−NH_3 profiles of (a) the freshly reduced MoP/γ-Al_2O_3 catalysts and (b) the representative deconvolution of the TPD−NH_3 profile of the $MoP_{(1)}$/Al sample.

Table 3. Acid Sites Concentration for Freshly Reduced Catalysts

	acid site concentration (mmol of NH_3 g_{cat}^{-1})			
sample	weak <500 K	medium 500−650 K	strong >650	total
$MoP_{(0.5)}$/Al	0.05	0.40	0.14	0.59
$MoP_{(1)}$/Al	0.08	0.27	0.22	0.57
$MoP_{(2)}$/Al	0.06	0.48	0.15	0.69
$MoP_{(3)}$/Al	0.06	0.39	0.17	0.62

[a] As deduced from amount of desorbed ammonia determined by TPD of NH_3. Adsorption of ammonia was performed at 353 K.

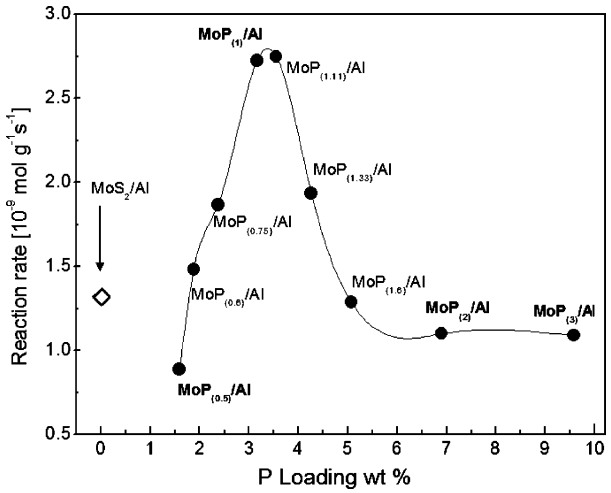

Figure 9. Comparison of the reaction rates after 100 h on-stream for MoP/γ-Al_2O_3 catalysts. For each catalyst, the DBT concentration in the feed was adjusted to obtain DBT conversion below 15%, $T = 553$ K and $P_{H_2} = 3.4$ MPa.

Al and $MoP_{(3)}$/Al catalysts were 0.22 and 0.17 mmol NH_3 g_{cat}^{-1}, respectively.

The catalytic response of the synthesized materials was verified in the gas-phase HDS reaction of DBT. P/Al catalyst was not active in the HDS reaction (data not shown here). The steady-state reaction rates of the MoP catalysts vs P content are compared in Figure 9 with that of the sulfided Mo/Al_2O_3 reference catalyst. Activity data were obtained by keeping DBT conversion below 15%. As seen in Figure 9, the activity of MoP catalysts went through a maximum with initial P content between 3 and 4 wt %. Thus, the monophosphide $MoP_{(1)}$/Al and $MoP_{(1.1)}$/Al catalysts reveal the largest HDS activities among the catalysts studied. As the CUS sites are considered to be active sites in the HDS reaction,[3,4] the presence of low valence state Mo detected by XPS technique for those catalysts might explain their high HDS activity. For the catalysts with initial P/Mo ratio higher than 1.1, HDS activity decreased to a P/Mo ratio of 2, which corresponds to 6.7 wt % P. A further increase in the P-content from 6.7 to 9.6 wt % had no subsequent effect on catalytic activity. Thus, the HDS activity of MoP/γ-Al_2O_3 catalysts in this study depends heavily on the P/Mo ratio being the optimal P/Mo ratio close to stoichiometric quantities. On the other hand, the marginal effect of P loading on the HDS activity of a model distillate feed over Ni_2P/SiO_2 systems was reported by Oyama et al.[28] This difference is most likely due to a mixture of DBT, quinoline, benzofuran, and tetralin used by these authors; the N-containing compounds are known to inhibit the HDS reaction. Indeed, in the absence of competitive adsorption of nitrogen compounds on the active sites, the thiophene HDS activity of the Ni_xP_y/Al_2O_3 and Ni_xP_y/SiO_2 systems was found to depend largely on the P/Ni molar ratio of the oxidic precursors with optimal activities achieved for catalysts containing pure Ni_2P and minimal excess of P.[25] In close agreement with other studies,[15,22] all MoP catalysts show larger activity than the sulfide MoS_2/Al_2O_3 reference sample (Figure 9). The most active $MoP_{(1)}$/Al sample was therefore doubly more so than the MoS_2 catalyst with the same Mo loading. The larger activity of MoP catalysts with respect to the MoS_2/Al_2O_3 sample can be explained by considering that the globular structure of the MoP phase might offer a larger density of active sites than the layered structure of the MoS_2 phase, as proposed by Oyama et al.[23]

The MoP was the major phase detected on the low-P-loading MoP/Al_2O_3 catalysts. Thermodynamically, the MoP phase is the most stable phosphide under the reduction conditions used here (hydrogen pressure of 3.1 MPa) and no P excess was necessary to yield MoP with a few phosphate species. Considering the EFTEM study (Figure

6), the activity decay of P-rich catalysts with respect to that with a P/Mo ratio close to 1 is because the polyphosphates or $AlPO_4$ phases might block the MoP particles, as shown in Scheme 2. This is consistent with the study by Oyama et al.,[23] who observed that an excess of phosphorus lowers the HDS activity of Ni_2P catalysts by blocking active sites. From the ^{31}P MAS NMR study, the decrease in activity of the P-rich samples comes from the formation of polyphosphates and $AlPO_4$ phase on the support surface. On the other hand, the low activity of $MoP_{(0.5)}/Al$, $Mo_{(0.6)}/Al$, $MoP_{(0.75)}/Al$ catalysts originated from a low density of MoP surface sites associated with a low P loading. The surface exposure of Mo species (Table 2) follows the same trend as catalytic activity data (Figure 9), indicating that the HDS reaction of DBT occurs on the active phases located on the support surface.

Hydrogen adsorption experiments were conducted to compare the H_2-uptake capacity of catalysts. Considering that alumina can adsorb hydrogen only after heating to 703 K in H_2 for several hours,[42−45] hydrogen adsorption on the support at 298 K is negligible. Hydrogen-uptake capacity and metal dispersion calculated from them are compiled in Table 2. As seen in this table, both H_2 chemisorption capacity and metal dispersion data generally follow the same trend as those of reaction rate: $MoP_{(1)}/Al \gg MoP_{(2)}/Al \approx MoP_{(0.5)}/Al \approx MoP_{(3)}/Al$. The critical role of metal−hydrogen bond formation in different hydrotreating reactions over MoP/Al_2O_3 catalysts was proven by Muetterties and Sauer.[9] Thus, the H_2 chemisorption capacity of the phases formed after precursor reduction at 1123 K seems to be the most important feature determining the HDS activity of the catalysts. The low H_2 uptake achieved by $MoP_{(0.5)}/Al$, $MoP_{(2)}/Al$, and $MoP_{(3)}/Al$ catalysts might explain their lower activity with respect to the $MoP_{(1)}/Al$ sample (Figure 9). The H_2 chemisorption data reported here for the alumina-supported MoP catalysts enabled us to calculate turnover frequencies (TOF). Considering TOF values, the intrinsic activity of the catalysts follows the trend: $MoP_{(1)}/Al$ (2.24×10^{-5} s^{-1}) > $MoP_{(3)}/Al$ (2.16×10^{-5} s^{-1}) > $Mo_{(2)}/Al$ (1.44×10^{-5} s^{-1}) ≈ $MoP_{(0.5)}/Al$ (1.39×10^{-5} s^{-1}). Assuming that the H atoms are transferred to the adsorbed S-containing molecule once they are activated under reaction conditions, it appears evident that such transfer is partly inhibited in the $MoP_{(3)}/Al$ sample. This is due to the presence of the $AlPO_4$ phase on the catalyst surface, and hence the reaction rate decreases although its TOF value is closer to that of the most active $MoP_{(1)}/Al$ sample. From these results, it appears possible to tune P content to maximize HDS activity.

For all the catalysts studied, the main product of HDS reaction over MoP/Al_2O_3 catalysts was biphenyl (ca. 85%). Other minor products were cyclohexylbenzene (ca. 14%) and 1,2,3,4-tetrahydrohydrodibenzothiophene (THDBT) (ca. 1%). Thus, regardless of P content, all the catalysts show the same

Scheme 3. Reaction Scheme for the HDS of DBT over Mo−P/γ-Al_2O_3 Catalyst

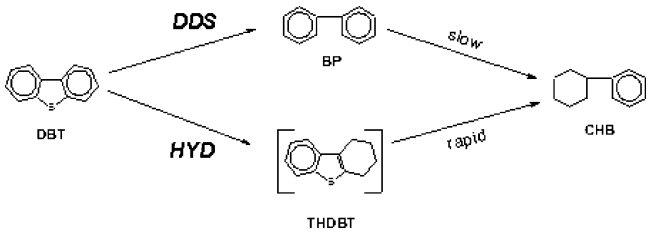

product distribution obtained at the same DBT conversion of 15%. On the basis of the experimental data, we derived the formal reaction network given in Scheme 3 for the HDS of DBT over MoP and MoS_2 catalysts. As seen in this scheme, the DBT compound is readily transformed by parallel DDS and HYD reaction pathways into biphenyl (BP) and cyclohexylbenzene (CHB), respectively. The latter is formed by the hydrogenation of one aromatic ring of DBT, followed by C−S bond cleavage of the THDBT. We were able to detect THDBT because the reaction temperature was thermodynamically far from its critical temperature when its formation became difficult (553 K vs 603 K).[45] As inferred from the low selectivity toward CHB (14%) and the absence of dicyclohexyl (DCH) formation, all catalysts show a lower capacity for hydrogenation than for C−S bond scission. Considering HRTEM results (Table 2), the possible explanation for the similar selectivity of all MoP/Al catalysts involves their similar morphology. The similar hydrogenation properties of all catalysts (including molybdenum sulfide catalyst) precluded the possibility of an acid-catalyzed reaction mechanism. In such a reaction mechanism, it is assumed that after hydrogen becomes dissociated at the metal site, the H atom spills over from the metal to the compounds strongly adsorbed on the acid site located in the close vicinity of the hydrogenation sites.[46] Indeed, the electronic effect in the HDS of DBT reaction, which could be induced by acid sites, has been reported to take place to a very low extent.[42−44,47−48]

Long-term experiments (100 h on-stream) were performed to study catalyst stability. The time on-stream behavior of all catalysts is shown in Figure 10. As seen in this figure, all MoP catalysts show good stability during 100 h of on-stream reaction. The absence of catalyst deactivation was observed previously for MoP catalysts.[19] However, contrary to literature reports,[19] the activity of the sulfide MoS_2/Al_2O_3 catalyst did not decrease with time on-stream up to 100 h (Figure 10). Apparently, S-poisoning of CUS sites does not occur. This could be explained by considering the dual effect of H_2S as promoter and inhibitor for HDS of DBT.[49] Farag et al.[49] observed that H_2S might simultaneously promote hydrogenation activity, which leads to an increase in overall activity, and inhibit the direct desulfurization route of the HDS of DBT reaction. However, further study is needed to

(42) Riseman, S. M.; Bandyopadhyay, S.; Massoth, F. E.; Eyring, E. M. *Appl. Catal.* **1985**, *16*, 29−37.
(43) Topsøe, N.-Y.; Topsøe, H.; Massoth, F. E. *J. Catal.* **1989**, *119*, 252−255.
(44) Topsøe, N.-Y.; Topsøe, H. *J. Catal.* **1993**, *139*, 641−651.
(45) Conner, W. C.; Pajonk G. M.; Teichner S. J. *Adv. Catal.* **1986**, *34*, 1−79.
(46) Farag, H.; Whitehurst, D. D.; Sakanishi, K.; Mochida, I. *Catal. Today* **1999**, *50*, 49−56.
(47) Castaño, P.; Pawelec, B.; Fierro, J. L. G.; Arandes, J. M.; Bilbao, J. *Fuel* **2007**, in press.
(48) Kurhinem, M.; Pakkanen, T. A. *Appl. Catal., A* **2000**, *192*, 97−103.
(49) Farag, H.; Sakanishi, K.; Kouzu, M.; Matsumura, A.; Sugimoto, Y.; Saito, I. *Catal. Commun.* **2003**, *4*, 321−326.

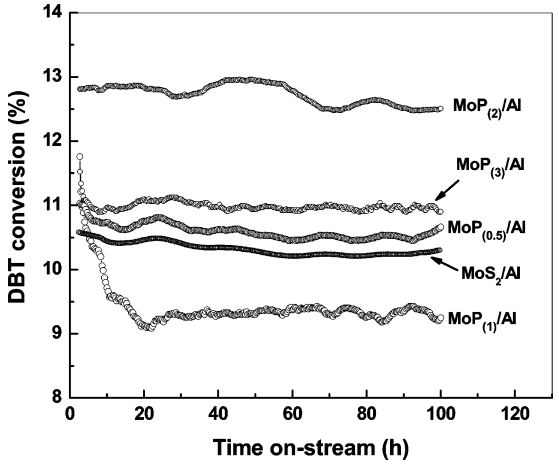

Figure 10. Time on-stream behavior of the MoP/γ-Al_2O_3 catalysts in HDS of DBT at 553 K and $P_{H_2} = 3.4$ MPa.

clarify the absence of deactivation of the MoS_2/Al sample under the reaction conditions used.

In this study, the absence of deactivation and similar selectivity in the HDS of DBT reaction of MoP/Al_2O_3 and MoS_2/Al_2O_3 catalysts indicate the simultaneous presence of both MoP and MoS_2 phases during on-stream operation. The MoS_2 species might be formed from MoP phase during the HDS reaction.[12,24] Indeed, the IR study of adsorbed CO performed by Wu et al.[24] confirmed the sulfidation of the surface of MoP/SiO_2 catalysts treated under a H_2S/H_2 mixture. The unique activity of MoP catalysts in hydrotreating reactions was explained previously by Stinner et al.[12] as being due to the simultaneous presence of both P and S atoms on the surface of catalysts. Moreover, it was reported that phosphate ions had a very significant effect on improving the thermal stability of γ-alumina with regard to sintering and phase transition to α-alumina.[41]

In short, this study has shown that molybdenum phosphide catalysts are more effective for the removal of sulfur during the desulfurization of DBT than a MoS_2/Al_2O_3 catalyst with the same Mo loading. In line with our previous study on sulfide CoMo catalysts,[50] the absence of correlation between the activity of molybdenum phosphide catalysts and their acidity was observed. This suggests that CUS sites may play a greater role than Brønsted acidity during DBT transformation.[50−52]

4. Conclusions

(i) The formation of the MoP phase after precursor reduction at 1123 K was confirmed by NMR, XPS, and HRTEM. These MoP phases with a well-defined globular crystalline structure were uniformly distributed on the surface of the mesoporous alumina (HRTEM, XPS). ^{31}P MAS−NMR studies pointed to the inhibition of $AlPO_4$ phase formation when stoichiometric amounts of Mo and P species are present on the catalyst surface.

(ii) The largest HDS activity was found for MoP(1)/Al and MoP(1.1)/Al in which the P/Mo molar ratio approaches the stoichiometric one. Irrespective of P-content, the MoP catalysts showed higher HDS activity than the sulfided MoS_2/Al_2O_3 sample with the same Mo loading. The HDS of DBT over all catalysts proceeds via the direct desulfurization (DDS) and hydrogenation (HYD) pathways, with the former being the main reaction route. The similar selectivity of molybdenum phosphide catalysts and the molybdenum sulfide one, as well as their high catalyst stability during 100 h of on-stream operation, indicate that both MoP and MoS_2 are active phases in the HDS of DBT reaction over MoP/γ-Al_2O_3 catalysts.

(iii) The globular morphology of the MoP phase, which displays a high H_2 adsorption capability, is found to be an important feature determining the HDS activity of the catalysts.

Acknowledgment. A.M.-C. and T.A.Z. are grateful to ICP−CSIC Spain and DEGEP, CONACyT, México, for financial support. The Spanish Ministry of Science and Technology is also acknowledged for funding the PPQ2002-11841-E project. Thanks are due to Prof. T. Halachev for valuable comments and suggestions. The authors are grateful to Eric Flores by the valuable technical assistance.

CM071814I

(50) Nava, R.; Ortega, R. A.; Alonso, G.; Ornelas, C.; Pawelec, B.; Fierro, J. L. G. *Catal. Today*. **2007**, in press (doi: 10.1016/j.cattod.2007.02.034).
(51) Perot, G. *Catal. Today* **2003**, *86*, 111−128.
(52) Lecrenay, E.; Sakanishi, K.; Nagamatsu, T.; Mochida, I.; Suzuka, T. *Appl. Catal., B* **1998**, *18*, 325−330.